Inorganic Chemistry

Article

pubs.acs.org/IC

Synthetic and Structural Study of the Coordination Chemistry of a *peri*-Backbone-Supported Phosphino-Phosphonium Salt

Matthew J. Ray, Michael Bühl, Laurence J. Taylor, Kasun S. Athukorala Arachchige, Alexandra M. Z. Slawin, and Petr Kilian*

School of Chemistry, EaStChem, University of St. Andrews, Fife, KY16 9ST, United Kingdom

Supporting Information

ABSTRACT: Coordination chemistry of an acenaphthene *peri*-backbone-supported phosphino-phosphonium chloride (**1**) was investigated, revealing three distinct modes of reactivity. The reaction of **1** with $Mo(CO)_4$(nor) gives the Mo(0) complex [(**1**)$Mo(CO)_4Cl$] (**2**), in which the ligand **1** exhibits monodentate coordination through the phosphine donor and the P−P bond is retained. $PtCl_2$(cod) reacts with the chloride and triflate salts of **1** to form a mononuclear complex [(**1**Cl)$PtCl_2$] (**3**) and a binuclear complex [((**1**Cl)$PtCl)_2$][2TfO] (**4**), respectively. In both of these complexes, the platinum center adds across the P−P bond, and subsequent chloride transfer to the phosphenium center results in phosphine-chlorophosphine bidentate coordination. [((**1**)$PdCl)_2$] (**5**) was isolated from the reaction of **1** and $Pd_2(dba)_3$ (dba = dibenzylideneacetone). Oxidative addition to palladium(0) results in a heteroleptic phosphine bridging phosphide coordination to the Pd(II) center. In addition, reaction of **1** with $BH_3{\cdot}SMe_2$ leads to the bis(borane) adduct of the corresponding mixed tertiary/secondary phosphine (**6**), with BH_3 acting as both a reducing agent and a Lewis acid. The new compounds were fully characterized, including X-ray diffraction. The ligand properties of **1** and related bonding issues are discussed with help of DFT computations.

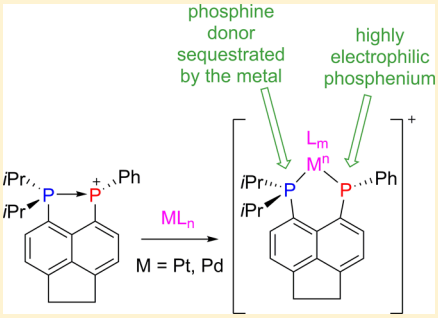

INTRODUCTION

As six-electron species, phospheniums, R_2P^+, can act as acceptors to suitable lone-pair donors. Phosphino-phosphoniums ($R_3P{\rightarrow}PR_2^+$) result from coordination of phospheniums by phosphines. Alternatively, phosphino-phosphoniums can be viewed as a class of quasi-phosphonium salts (PR_4^+) having a phosphine ($-PR_2$) group as one of its four substituents (see onium form in Scheme 1). Although the onium form arguably describes the bonding more accurately, the dative description is useful, for example, when considering the reactivity of phosphino-phosphoniums in which the phosphine is exchanged with another donor. There are multiple examples of such donor exchange in the literature (see below).

Scheme 1. Onium and Dative Resonance Structures of Phosphino-Phosphoniums

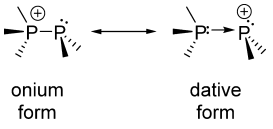

Phosphino-phosphonium salts $[R_3P^+{-}PR_2]^+[X]^-$ were first reported in 1959 as products of the reaction of a diphosphine with an alkyl iodide.[1] Later, their preparation from trialkylphosphines and chlorophosphines was studied rather extensively.[2] The discovery that phosphino-phosphonium salts are also the products of coordination of phosphines to free phosphenium salts was very important in the development of their synthetic accessibility.[3] A small number of further reports on these reactions followed,[4−6] but it was not until Burford began work on phosphino-phosphoniums that the synthetic methodology became well developed and the range of functional groups used in the $[R_3P{-}PR_2]^+$ framework was dramatically extended.[7] The new motifs included multi-phosphorus atom chains[8] and rings.[9]

Aside from preparation of 1,2-diphosphoniums,[10] little was reported on the reactivity of phosphino-phosphoniums. Nonetheless, experimental evidence for the dative character of the P−P bond has been provided in a series of ligand-exchange reactions in which the phosphine component was replaced by another phosphine or a carbene (for selected examples, see Scheme 2).[11]

The exchange reactions demonstrate the lability of the P−P bond in phosphino-phosphoniums and show the potential for further discovery of diverse reactivity. It would be expected that phosphino-phosphoniums demonstrate complex and varied coordination chemistry due to the presence of two differing phosphorus centers. Notably, the ambiphilic phosphenium component should become available for further coordination via sequestration of the phosphine's lone pair.

A surprisingly limited number of reports on transition metal complexes of phosphino-phosphoniums has appeared in the

Received: May 16, 2014
Published: July 29, 2014

   dx.doi.org/10.1021/ic501142v | *Inorg. Chem.* 2014, 53, 8538−8547

Scheme 2. Donor Exchange in Phosphino-Phosphoniums

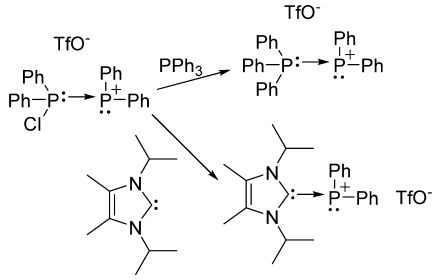

literature. Schmutzler reported complex **A** in which the phosphino-phosphonium acts as a (cationic) monodentate ligand to a tungsten(0) center (Scheme 3).[12] The same group

Scheme 3. Metal Complexes of Phosphino-Phosphoniums Synthesized by Schmutzler[12,13]

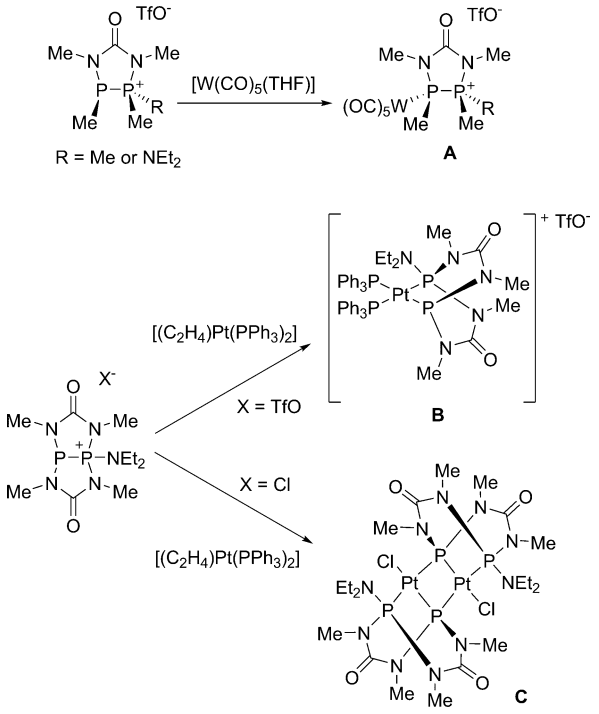

also investigated the reaction of bicyclic phosphino-phosphonium salts with a Pt(0) complex, which resulted in oxidative P−P bond cleavage to form chelating phosphine-phosphido Pt(II) complexes **B** and **C** (Scheme 3).[13]

Thomas reported a series of complexes of phosphino-phosphonium pincer ligand **D**, in which the central motif consists of N-heterocyclic phosphenium (NHP) group (Scheme 4).[14] Several phosphine-phosphido complexes (**E**) were synthesized from **D**.[15] Additionally, rare bridging phosphine-phosphenium complexes **F** were reported in which the central phosphorus atom attains semibridging NHP^+ arrangement with metal atoms in oxidation state 0.[15] Interestingly, related M(I) phosphine-phosphido binuclear complexes **G** were obtained by reduction of the appropriate halogenated precursors similar to **E** with sodium amalgam.[16] Phosphine-chlorophosphine complex **H** was formed via migration of a chloride from platinum to the Lewis acidic phosphenium center.[14]

Scheme 4. Metal Complexes Synthesized from Phosphino-Phosphonium Salt D by Thomas[14−16]

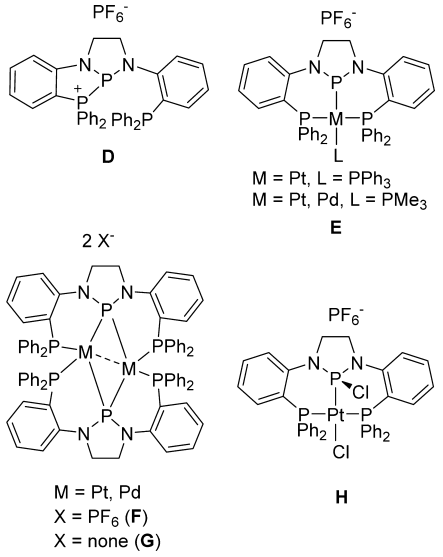

Modification of phosphine functionalities in order to tune their steric and electronic properties has been a major research area for some years, and a phosphine center being directly bound to a cationic phosphonium center represents a tentatively explored electronic environment in the context of coordination chemistry, particularly considering that tertiary phosphines with a net positive charge are relatively unexplored compared with negatively charged species.[17,18] There is also considerable interest in phosphenium coordination chemistry,[19] as phospheniums are isolobal to two archetypal ligands: carbenes and the nitrosonium cation. Our group has previously reported *peri*-substituted phosphino-phosphoniums and 1,2-diphosphoniums,[10b,20] and more recently we have used the principles of earlier work[21] to synthesize *peri*-substituted phosphino-phosphoniums directly from dichlorophosphines.[22] Here, we report a series of coordination complexes prepared from a *peri*-substituted phosphino-phosphonium salt **1**.

RESULTS AND DISCUSSION

Bonding in Phosphino-Phosphonium 1. The phosphino-phosphonium chloride salt **1** was used as the starting point for all of the reactions presented in this work. An efficient synthesis and a range of reactivity of **1** was reported by us recently.[22] **1** has an ionic structure in the crystal; it consists of a complex phosphino-phosphonium cation and a chloride counterion, as confirmed by single-crystal X-ray diffraction. The P−P bond length in **1** is 2.2347(9) Å, typical of a single bond (normal range 2.20 ± 0.05 Å). $^{31}P\{^1H\}$ NMR data indicate the ionic phosphino-phosphonium structure is retained also in the chloroform solution; the spectrum consists of two doublets at δ_P −34.5 (PPh) and 60.0 ppm ($PiPr_2$), $^1J_{PP}$ = 303 Hz. These chemical shifts correspond well with the phosphine and phosphonium environments of the ionic structure, as opposed to phosphine and chlorophosphine environments in the (nonionic) molecular structure.[22]

In order to obtain further insight into the bonding in **1**, the nature of the P−P bond was probed through natural population (NPA) and natural bond orbital (NBO) analysis at the B3LYP/6-31+G* level. The localized P−P bonding NBO is almost equally shared between both phosphorus atoms (Figure 1).

dx.doi.org/10.1021/ic501142v | Inorg. Chem. 2014, 53, 8538−8547

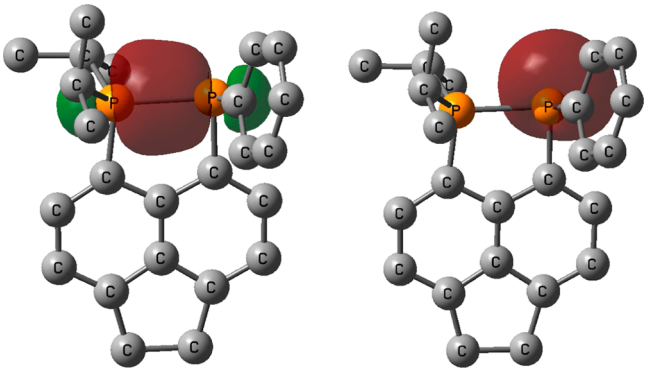

Figure 1. Localized NBOs in **1** showing the P−P bonding orbital (left) and the lone pair on phosphine center (right) at the B3LYP level; H atoms are omitted for clarity.

Natural charges at phosphorus atoms are +0.69 (PPh) and +1.27 (P(iPr$_2$)). A computed Wiberg bond index (WBI) is 0.89, indicative of a rather normal covalent single bond.[23] The computations thus indicate that the bonding situation is close to that described by an onium Lewis structure with a regular shared P−P bond and a formal positive charge on the PiPr$_2$ phosphorus atom.

To probe the bonding through alternative means, we resorted to the seminal paper on donor−acceptor versus normal bonding by Haaland.[24] Here, the chemical bond is classified as dative if minimum-energy rupture proceeds heterolytically, whereas for a normal (covalent) bond, minimum-energy rupture proceeds homolytically. Because in **1** the phosphonium and phosphine functionalities are tethered through the rigid organic backbone (preventing a simple dissociation), we had to resort to an unbridged model phosphino-phosphonium [iPr$_2$PhP−PPh$_2$]$^+$ for our computations. The heterolytic and homolytic P−P dissociation of the model cation are described in eqs 1 and 2.

$$[i\mathrm{Pr}_2\mathrm{PhP}-\mathrm{PPh}_2]^+ \rightarrow \mathrm{P}i\mathrm{Pr}_2\mathrm{Ph} + \mathrm{PPh}_2^+ \quad (1)$$

$$[i\mathrm{Pr}_2\mathrm{PhP}-\mathrm{PPh}_2]^+ \rightarrow \mathrm{P}i\mathrm{Pr}_2\mathrm{Ph}^{\bullet+} + \mathrm{PPh}_2^{\bullet} \quad (2)$$

In terms of the raw gas-phase B3LYP energies, heterolytic dissociation (eq 1) is favored over the homolytic one (eq 2) by 11.1 kcal mol^{-1}, indicating that there is a case for assigning dative character to the P−P bond. We note that the energy difference reflects stabilization of the positive charge in PPh$_2^+$ (eq 1) via delocalization over two phenyl rings, whereas in cation radical PiPr$_2$Ph$^{\bullet+}$ (eq 2), there is only one phenyl ring available for this. In line with this, the computed natural charge on the phosphorus atom drops from +1.37 in PiPr$_2$Ph$^{\bullet+}$ to +1.08 in PPh$_2^+$. Our findings are consistent with theoretical study by Pietschnig,[25] in which model phosphine-phosphoniums with π-donating groups on the phosphenium were classified as dative according to Haaland's criterion.

Coordination Chemistry of Phosphino-Phosphonium 1. As an entry into the coordination chemistry of **1**, its reaction with [Mo(CO)$_4$(nor)] (nor = norbornadiene) in CH$_2$Cl$_2$ was carried out. This gave overall electroneutral complex [(**1**)Mo(CO)$_4$Cl] (**2**) as a yellow powder in 75% yield. The $^{31}\{^1\mathrm{H}\}$ NMR spectrum of **2** consists of two doublets at δ_P 36.0 (PPh) and 52.4 (PiPr$_2$) ppm ($^1J_{PP}$ = 250.4 Hz). Hence, the PhP signal has shifted dramatically to higher frequency on coordination to the molybdenum center (by ∼70 ppm), whereas the magnitude of the $^1J_{PP}$ coupling constant is only slightly smaller in **2** than **1**, still consistent with a formal P−P bond. The solid-state structure of **2** confirms monodentate coordination of **1** through P1 as well as coordination of the chloride *cis* to the phosphorus donor atom to form an octahedral molybdenum complex (Figure 2 and Tables 2−4).

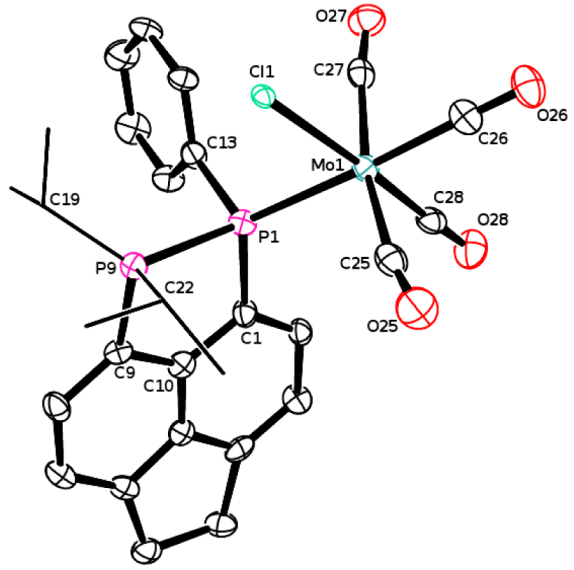

Figure 2. Molecular structure of **2**. Co-crystallized molecule of THF and hydrogen atoms are omitted for clarity. *i*Pr groups are shown in wireframe for clarity.

The formation of **2** resembles the phosphino-phosphonium reactivity observed by Schmutzler in the formation of complex **A** (Scheme 3).[12] The P−P bond remains intact, whereas the phosphino-phosphonium behaves as a tertiary phosphine with the phosphonium acting as an innocent cationic charge carrying substituent at the phosphorus donor atom. The coordination of the chloride to the molybdenum center in **2** makes **1** an unusual example of an ion pair in which both components behave as ligands. The P−Mo bond length in **2** is 2.5283(16) Å, only slightly elongated versus that in [Mo(CO)$_5$PPh$_3$] (2.506(1) Å).[26] The P−P bond length in **2** is 2.271(3) Å, again only modestly elongated compare to that in **1** (2.2347(9) Å).[22]

The CO stretching frequencies of **2** observed in its IR spectrum give an indication of the electronic properties of monodentate cationic ligand **1**. In Table 1, the IR data of

Table 1. CO Stretching Frequencies for [LMo(CO)$_4$Cl] Complexes

	υCO (cm^{-1})			
[Mo(CO)$_5$Cl][NEt$_4$]	2064	1913		1871
[(Ph$_3$P)Mo(CO)$_4$Cl][NEt$_4$]	2003	1890	1875	1822
[((*i*PrO)$_3$P)Mo(CO)$_4$Cl][NEt$_4$]	2005	1890	1880	1833
[(**1**)Mo(CO)$_4$Cl] (**2**)	2019	1912	1893	1832

electroneutral complex **2** are compared with those of the related (ionic) complexes [Mo(CO)$_5$Cl][NEt$_4$],[27] *cis*-[((*i*PrO)$_3$P)Mo(CO)$_4$Cl][NEt$_4$], and *cis*-[(Ph$_3$P)Mo(CO)$_4$Cl][NEt$_4$].[28] The large decrease in stretching frequency compared with [Mo(CO)$_5$Cl][NEt$_4$] indicates that **1** is more basic than CO. However, the fact that the PPh$_3$ and P(OiPr)$_3$ complexes have lower CO stretching frequencies than **2** indicates that **1** is a weaker donor than both of these (charge

dx.doi.org/10.1021/ic501142v | Inorg. Chem. 2014, 53, 8538−8547

neutral) ligands, presumably due to the overall positive charge of the phosphino-phosphonium ligand.

Reaction of **1** with $PtCl_2(cod)$ in CH_2Cl_2 gave the phosphine-chlorophosphine platinum(II) dichloride complex **3** as a pale yellow solid in quantitative yield. The $^{31}P\{^1H\}$ NMR spectrum of **3** exhibits two doublets ($^2J_{PP}$ = 26.4 Hz) with ^{195}Pt satellites centered at δ_P 12.8 (P*i*Pr$_2$, $^1J_{PPt}$ = 3201 Hz) and 41.9 (PPhCl,$^1J_{PPt}$ = 3836 Hz) ppm. $^{195}Pt\{^1H\}$ NMR consists of a doublet of doublets at δ_{Pt} = −4326 ppm, with the $^1J_{PPt}$ coupling constants identical with those observed in the $^{31}P\{^1H\}$ NMR spectrum.

Given the ion-separated structure of **1**, it is reasonable to assume that the formation of **3** proceeds through bidentate coordination of **1** to the platinum center followed by a chloride attack of the phosphenium center. Increase of Lewis acidity of the phosphenium atom on coordination to the platinum center (see Scheme 5) is likely to facilitate the subsequent co-

Scheme 5. Tentative Mechanism of the Formation of Complexes 3 and 4

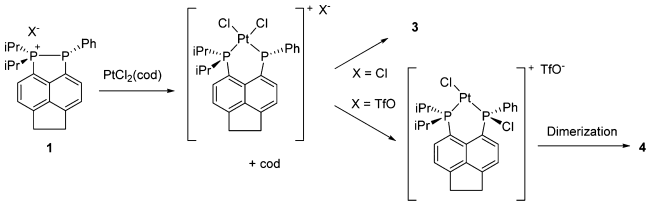

ordination of the chloride. Notably, the observed reactivity leading toward **3** is more compatible with the dative bonding model rather than the onium one (see Scheme 1).

The solid-state structure of **3** is shown in Figure 3, and data are presented in Tables 2−4. The geometry around platinum is square planar, with the *cis* angles ranging from 87.6(1) to 94.6(1)°. The P1···P9 distance in **3** is 3.26 Å, and a positive

Scheme 6. Syntheses Reported in This Article

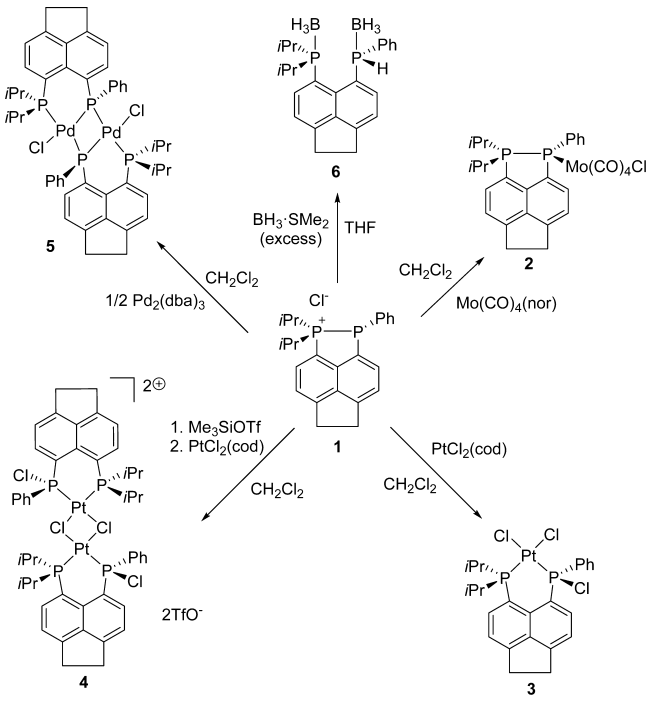

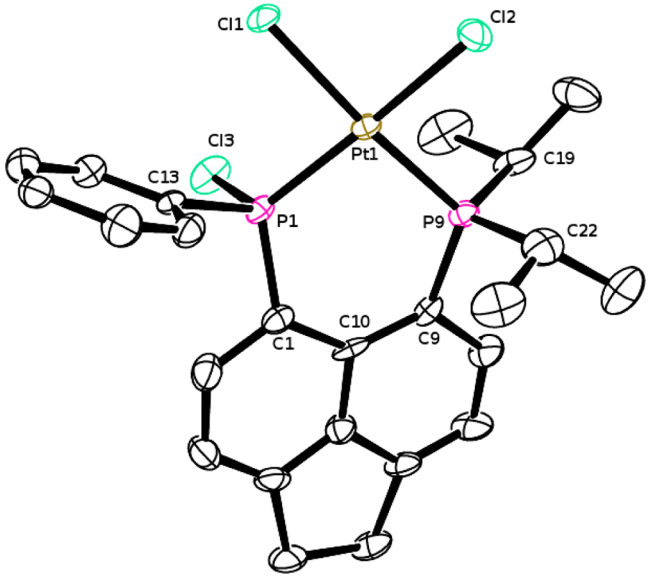

Figure 3. Molecular structure of **3**. Hydrogen atoms are omitted for clarity.

splay angle of +18(1)° is observed (see Figure 4 for a definition). Coordination of platinum introduces some angular

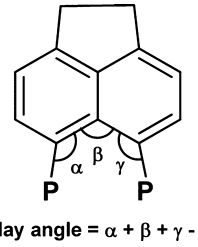

Figure 4. Definition of a splay angle.

strain to the *peri* region; notably, both phosphorus atoms are bending out of plane on opposite sides of the acenaphthene ring quite significantly (P1 0.59 Å; P9 0.37 Å).

Observation of the attack of the chloride ion at P1 during the formation of **3** inspired us to investigate this reaction with a less coordinating anion in place of chloride. To this end, **1** was reacted with Me_3SiOTf to give the anion-exchange product, a triflate salt of **1**. The solution of the triflate salt was added to $PtCl_2(cod)$ to give a pale yellow solution. Layering of the solution with hexane led to formation of **4** as a white precipitate (95% yield) as well as crystals suitable for X-ray crystallography. Once precipitated, **4** has very poor solubility in common organic solvents, which hindered its study by solution NMR spectroscopy. Nonetheless, two doublets ($^2J_{PP}$ = 28.0 Hz) at δ_P 11.3 ($^1J_{PPt}$ = 3409 Hz) and 38.5 ppm ($^1J_{PPt}$ = 3582 Hz) were identified in the $^{31}P\{^1H\}$ NMR spectrum as those belonging to **4**. The ^{31}P NMR spectrum of **4** is thus very similar to that of **3**, with the exception of $^1J_{PPt}$ coupling constants which differ significantly, indicating changes in the Pt coordination sphere. Signals in ^1H NMR of **4** are broad and therefore difficult to interpret. We were unable to obtain $^{13}C\{^1H\}$ or ^{195}Pt NMR spectra of **4** due to its poor solubility.

The solid-state structure of **4** (Figure 5 and Tables 2−4) shows it to be a dicationic dimer of **3**, with the two bis(phosphine) units connected via two bridging chloride ligands. The dication adopts crystallographic C_i symmetry, with

dx.doi.org/10.1021/ic501142v | Inorg. Chem. 2014, 53, 8538−8547

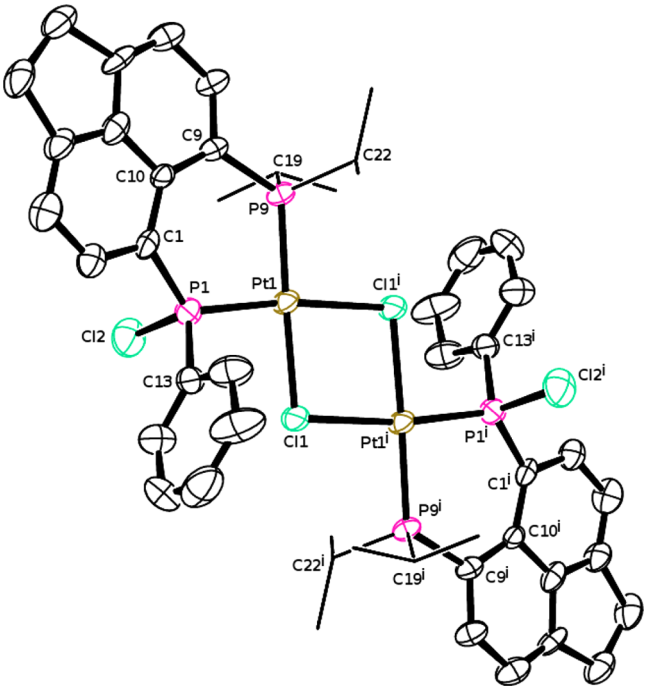

Figure 5. Molecular structure of the dication of **4**. Triflate counterions, two cocrystallized molecules of CH_2Cl_2, and hydrogen atoms are omitted for clarity. *i*Pr groups are shown in wireframe for clarity.

the inversion center located in the midpoint of the Pt_2Cl_2 ring. The dication is charge-balanced by two triflate counterions. The geometry around the platinum center shows only relatively small deviations from the ideal square planar *cis* angles [82.03(9)−94.36(9)°]. The P1···P9 distance is 3.24 Å, very similar to that found in **3**, as is the splay angle [+19.9(7)°]. The central Pt_2Cl_2 ring is planar, with the two bis(phosphine) ligands positioned *trans* with respect to each other.

The formation of **4** is postulated to proceed in a similar manner to that of **3** (Scheme 5); in the first step, **1** undergoes bidentate coordination to platinum, which is followed by migration of a chloride ligand from the platinum center to the phosphenium. The resulting cationic three-coordinate platinum(II) complex finally dimerizes to **4**.

Reactivity similar to that observed by us was reported recently by Thomas;[14] reaction of their N-heterocyclic phosphenium pincer ligand with $PtCl_2$(cod) gave a product of chloride ligand migration from platinum to the phosphenium center (see **H** in Scheme 4).

In order to investigate the reactivity of our phosphino-phosphonium toward electron-rich metal fragments, we carried out the reaction of **1** with [Pd_2(dba)$_3$]. The reaction at room temperature gave the dimeric complex **5** as a bright yellow solid in 19% yield. $^{31}P\{^1H\}$ NMR of **5** revealed an AA′XX′ spin system with $\delta_{P(X)}$ 14.7 and $\delta_{P(A)}$ −176.6 ppm (A, A′ = P*i*Pr$_2$; X, X′ = PPh). The large shift of PPh phosphorus to low frequency (by 142 ppm vs **1**) strongly indicates that two-electron reduction of the phosphenium to a phosphide has taken place, which is accompanied by oxidation of palladium from Pd(0) to Pd(II). **5** exhibits large magnitude phosphine-phosphide coupling constants as well as small phosphide-phosphide and phosphine-phosphine couplings (*trans*-$^2J_{AX}$ = 322.0 Hz, *cis*-$^2J_{AX}$ = 140.0 Hz, $^2J_{XX'}$ = 4.6 Hz, $^4J_{AA'}$ = 2.2 Hz).

The solid-state structure of **5** is shown in Figure 6, and data are given in Tables 2−4. The molecule adopts crystallographic

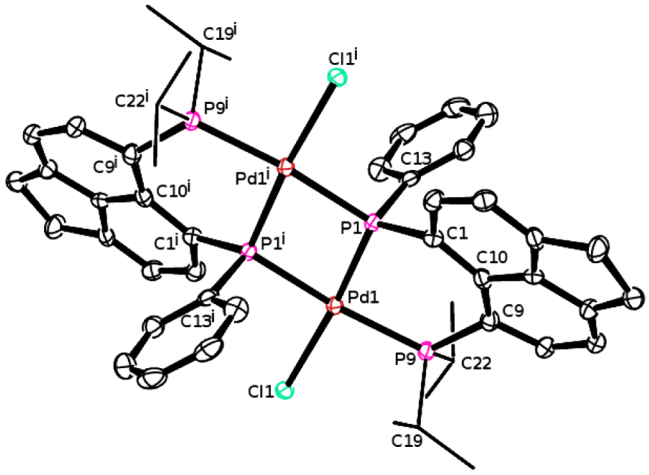

Figure 6. Molecular structure of **5**. Two cocrystallized molecules of CH_2Cl_2 and hydrogen atoms are omitted for clarity. *i*Pr groups are shown in wireframe for clarity.

C_i symmetry, with the inversion center located in the midpoint of the Pd_2P_2 ring. The coordination sphere of each metal center comprises a phosphine (P9), a terminal chloride, and two bridging phosphido ligands (P1 and P1^i). The P_2Pd_2 ring is planar, with the P1−Pd1−P1^i angle being mildly acute (77.48(6)°), leading to a Pd1···Pd1^i distance of 3.58 Å. The structural parameters of the *peri*-region in **5** are quite similar to those of **3** and **4**: the P1···P9 distance is 3.29 Å, and the splay angle is +15.5(5)°.

It is of interest to compare the bonding in **5** with that in a related dicationic dimeric palladium complex **F** reported recently by Thomas.[15] Similar to **5**, **F** was obtained by the reaction of an ionic phosphino-phosphonium ligand with a Pd(0) source ((Pd(PPh$_3$)$_4$). However, the bonding in **F** is rather dissimilar to that in **5**. In **F**, the bonding is described as NHP$^+$ phosphenium ligand being asymmetrically bonded to two Pd atoms in a "semibridging NHP arrangement" with one double and one single P−Pd bond, with Pd(0) centers possessing tetrahedral geometry.[15,19] In **5**, the Pd−P bond lengths for the phosphido phosphorus atoms differ slightly (2.2406(17) and 2.3504(18) Å), although they are both consistent with a single Pd−P bond character. The geometry around the phosphido atoms (P1 and P1^i) in **5** is close to tetrahedral, as expected for a μ^2-bridging phosphido ligand. The palladium centers adopt distorted square planar geometry, consistent with a d^8 configuration (i.e., Pd(II)). The P−Pd bond lengths in **5** indeed correspond well with those found in Pd_2P_2 metallacycles with bridging phosphido ligands.[29,30] In conclusion, the structural as well as NMR arguments strongly support the interpretation of bonding in **5** as a pyramidal phosphido Pd(II) complex. The formation of **5** is likely to proceed via oxidative addition of the P−P bond to the Pd(0) fragment and subsequent coordination of Pd by a chloride ligand.

In order to investigate reactivity of **1** toward an archetypal main group Lewis acid, we performed a reaction of **1** with an excess of BH_3·SMe_2. The reaction proceeds with BH_3-mediated reduction to give a bis(borane) adduct **6**, which was obtained after workup as a yellow oil in quantitative yield (Scheme 6). The $^{31}P\{^1H\}$ NMR spectrum of **6** exhibited broad singlets at δ_p −6.6 (PHPh) and 39.4 ppm (P*i*Pr$_2$). The ^{31}P NMR spectrum consisted of a broad doublet at −6.6 ($^1J_{PH}$ = 376 Hz) and a

dx.doi.org/10.1021/ic501142v | *Inorg. Chem.* 2014, 53, 8538−8547

broad singlet at 39.5 ppm, corresponding to the secondary and tertiary phosphine centers, respectively. Reaction optimization showed that complete conversion from **1** to **6** could not be achieved with less than 4 equiv of $BH_3{\cdot}SMe_2$: smaller amounts yielded mixtures of **1** and **6** but no additional products, as indicated by ^{31}P NMR. This suggests that P−P bond cleavage is the sole mode of reactivity in this case. Compound **6** is rather thermally labile. Attempts to remove traces of unreacted $BH_3{\cdot}SMe_2$ from the crude product via mild heating in vacuo resulted in partial decomposition (as monitored by ^{31}P NMR). This prevented obtaining good microanalysis data. The crude oily product obtained after stripping off the reaction solvent at ambient temperature was used to obtain all other characterization data (except for X-ray, see below).

Few crystals of **6** suitable for X-ray diffraction were obtained from cold MeCN. The molecular structure is shown in Figure 7, with data in Tables 2−4. The structure of **6** shows significant

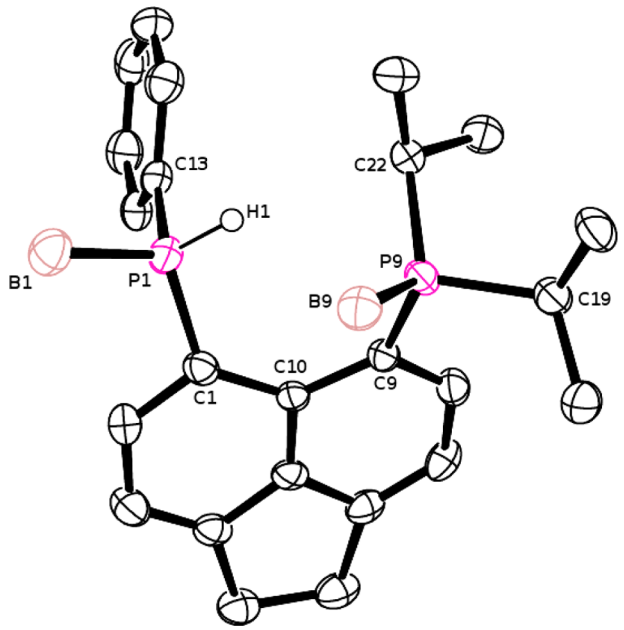

Figure 7. Molecular structure of **6**. Co-crystallized molecule of MeCN and carbon- and boron-bound hydrogen atoms are omitted for clarity.

strain in the *peri* region, with the phosphorus groups significantly bending away from each other and with a P1···P9 distance of 3.61 Å and a large positive splay angle of +24.4(4)°. Phosphorus atoms are displaced out of the mean plane of the acenaphthene ring significantly (0.48 Å for P1 and 0.82 Å for P9). Both phosphorus centers have distorted tetrahedral geometries.

In the formation of **6**, BH_3 is serving as both a reducing agent to the phosphonium and a Lewis acid to the resulting bis(phosphine), which is reminiscent of the role $NaBH_4$ plays in the reduction of chiral chlorophosphoniums in a recent report by Gilheany.[31] Notably, related reduction of **1** with $LiAlH_4$ also resulted in P−P bond cleavage, giving the parent phosphine Acenap($PiPr_2$)(PPhH) (Acenap = acenaphthene-5,6-diyl).[22] In contrast, a $GaCl_3$ adduct of an intact phosphino-phosphonium was reported by Burford.[32]

CONCLUSIONS

The phosphino-phosphonium **1** displays an array of distinct coordinative modes, although a phosphenium complex was not obtained in any of the studied reactions. This is expected, as the all-carbon character of **1** results in lesser electronic stabilization of the positively charged phosphenium than one would expect, for example, for NHP-type phosphino-phosphonium salts.

In the Mo complex **2**, the P−P bond is retained; hence, the mechanistic formation of **2** is conveniently described using the onium form of **1**. In all other metal complexes (**3**−**5**), the coordination proceeds with metal insertion into the P−P bond, which is mechanistically more in accord with the dative form of **1**. The formation of **3** and **4** can be readily explained by a chloride transfer to the phosphenium center, whose electrophilicity is augmented by sequestration of the phosphine donor as well as the metal coordination. For **5**, the transfer of a pair of electrons from electron-rich palladium(0) to an electron-deficient phosphenium seems more explicable than the alternative reduction of a chlorophosphine group followed by chloride transfer to the palladium. Hence, we conclude that **1** displays coordination behavior consistent with both onium and dative forms. Formally, the formation of complexes **3**−**5** involves phosphine/phosphenium transfer (to the metal fragments), thus paralleling the ligand transfer (main group) chemistry of phosphino-phosphoniums (Scheme 7). Sequestration of the phosphine donor by the metal results in a highly electrophilic phosphenium motif. This undergoes subsequent reaction: either halogen capture or two-electron reduction.

A different reactivity again is observed with prototypical main group Lewis acid borane, which in reaction with **1** acts as both a

Table 2. Selected Bond Lengths (Å) and Angles (deg) for 2·THF, 3, 4·2CH_2Cl_2, 5·2CH_2Cl_2, and 6·MeCN

2·THF			
C1−P1	1.835(7)	Mo1−Cl1	2.6013(19)
P1−Mo1	2.5283(16)	C9−P9	1.792(7)
P1−Mo1−Cl1	84.57(6)		
C9−P9−P1	96.6(3)	C1−P1−P9	90.7(3)
P9−P1−Mo1	121.90(9)	Mo1−P1−C13	114.89(19)
3			
C1−P1	1.799(13)	C9−P9	1.828(11)
Pt1−P1	2.186(3)	Pt1−P9	2.241(4)
Cl3−P1	2.050(4)		
P1−Pt1−P9	94.63(11)	Cl1−Pt1−Cl2	88.21(11)
4·2CH_2Cl_2			
C1−P1	1.759(7)	C9−P9	1.806(8)
Pt1−P1	2.186(3)	Pt1−P9	2.236(3)
Pt1−Cl1	2.405(3)	Pt1−$Cl1^i$	2.380(3)
Cl2−P1	1.995(5)	Pt1−Cl1−$Pt1^i$	97.97(11)
P1−Pt1−Cl1	89.92(9)	P9−Pt1−Cl1	173.84(9)
P1−Pt1−$Cl1^i$	170.96(10)	P9−Pt1−$Cl1^i$	93.99(9)
Cl1−P−$Cl1^i$	82.03(9)	P1−Pt1−P9	94.36(9)
5·2CH_2Cl_2			
C1−P1	1.822(6)	C9−P9	1.820(6)
Pd1−P1	2.2406(17)	$Pd1^i$−P1	2.3504(18)
Pd1−P9	2.3077(18)	Pd1−Cl1	2.3908(16)
P1−Pd1−$P1^i$	77.48(6)	P9−Pd1−P1	92.76(6)
P1−$Pd1^i$−$Cl1^i$	96.50(6)	P9−Pd1−Cl1	92.77(6)
P1−Pd^i−$P9^i$	167.10(6)	Pd1−P1−$Pd1^i$	102.52(7)
6·MeCN			
C1−P1	1.807(4)	C9−P9	1.834(5)
B1−P1	1.925(5)	B9−P9	1.944(5)
H1−P1	1.202(17)		
C1−P1−B1	116.48(19)	B1−P1−H1	108.8(15)
C1−P1−H1	108.9(14)	C9−P9−B9	112.55(19)

dx.doi.org/10.1021/ic501142v | *Inorg. Chem.* 2014, 53, 8538−8547

Table 3. *peri* Distances (Å), Splay Angles (deg), and Out-of-Plane Displacements (Å) for 2·THF, 3, 4·2CH_2Cl_2, 5·2CH_2Cl_2, and 6·MeCN[a]

	2·THF	3	4·2CH_2Cl_2	5·2CH_2Cl_2	6·MeCN
P1···P9	2.271(3)	3.26	3.24	3.29	3.61
splay angle	−8.5(6)	+18(1)	+19.9(7)	+15.5(5)	+24.4(4)
out-of-plane displacement (P1)	0.056	0.586	0.272	0.345	0.478
out-of-plane displacement (P9)	0.305	0.367	0.214	0.766	0.816

[a]See Figure 4 for the definition of a splay angle.

Scheme 7. Formation (and Fate) of the Phosphenium Center via Coordination of Phosphino-Phosphonium 1 to the Metal Fragment

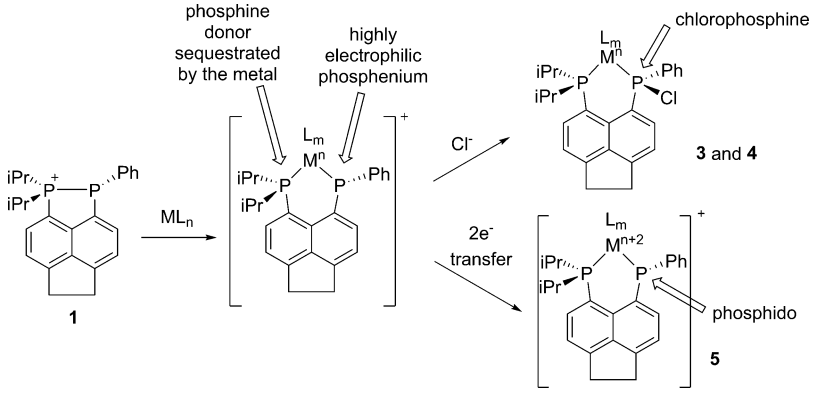

reducing reagent (hydride source) and a Lewis acid to give the bis(borane) adduct of the corresponding mixed tertiary/secondary phosphine **6**.

EXPERIMENTAL SECTION

General Procedures. All experiments were carried out in standard Schlenk glassware. Solvents were dried on an MBraun solvent purification system and stored over molecular sieves prior to use. 5-Bromo-6-diisopropylphosphinoacenaphthene,[21] phosphino-phosphonium chloride **1**,[22] and $PtCl_2$(cod)[33] were prepared according to literature procedures. Where possible, new compounds were fully characterized by ^{31}P, $^{31}P\{^1H\}$, ^1H, and $^{13}C\{^1H\}$ NMR, including measurement of $^1H\{^{31}P\}$, H−H DQF COSY, H−P HMQC, H−C HSQC, and H−C HMBC experiments. Measurements were performed at 25 °C unless otherwise indicated; 85% H_3PO_4 was used as an external standard in ^{31}P, TMS was used as an internal standard in ^1H and ^{13}C NMR, and aqueous Na_2PtCl_6 was used as an external standard in ^{195}Pt NMR. The NMR numbering scheme for **2**−**6** is shown in Figure 8.

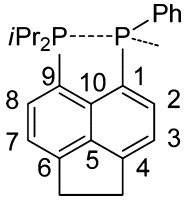

Figure 8. NMR numbering scheme for **2**−**6**.

[(1)Mo(CO)$_4$Cl] Complex (2). **1** (0.20 g, 0.484 mmol) in CH_2Cl_2 (8 mL) was added to [Mo(CO)$_4$(nor)] (0.16 g, 0.532 mmol) in CH_2Cl_2 (2 mL) at room temperature, and the mixture was stirred for 16 h. The resulting brown suspension was filtered to remove solids to give a dark orange solution, from which volatiles were removed in vacuo. The resulting orange oil was extracted with MeCN (2 mL), and volatiles were removed in vacuo to give **2** as a yellow solid (0.225 g, 75% yield). Orange crystals suitable for X-ray crystallography were grown from THF at 2 °C. EA (%) calcd for $C_{28}H_{27}ClMoO_4P_2$: C, 54.17; H, 4.38. Found: C, 54.10; H, 4.47. ^1H NMR (300.1 MHz, CD_2Cl_2): δ 0.67−0.94 (m, 6H, 2 × *i*Pr CH_3), 1.37−1.61 (m, 6H, 2 × *i*Pr CH_3), 2.48−2.65 (m, 1H, *i*Pr CH), 3.66 (s, 4H, 2 × CH_2), 3.82−3.97 (m, 1H, *i*Pr CH), 7.26−7.48 (m, 5H, 5 × Ph CH), 7.65−7.73 (m, 1H, H7), 7.75−7.82 (m, 1H, H3), 7.86 (t, 1H, ^3J = 7.6 Hz, H8), 8.4−8.5 (m, 1H, H2); $^{13}C\{^1H\}$ NMR (67.9 MHz, CD_2Cl_2): δ 16.8 (s, *i*Pr CH_3), 17.4 (d, $^2J_{CP}$ = 6.1 Hz, *i*Pr CH_3), 18.2 (s, *i*Pr CH_3), 19.3 (s, *i*Pr CH_3), 25.0 (d, $^1J_{CP}$ = 24.7 Hz, *i*Pr CH), 26.2−26.9 (m, *i*Pr CH), 31.8 (s, CH_2), 32.4 (s, CH_2), 122.7 (d, $^3J_{CP}$ = 9.3 Hz, C7), 123.6 (d, $^3J_{CP}$ = 10.1 Hz, C3), 129.8 (d, $^2J_{CP}$ = 9.3 Hz, *o*-Ph), 132.4 (s, C8), 134.5 (s, *m* or *p*-Ph), 134.7 (s, *m* or *p*-Ph), 135.1 (s, C2), 137.1−137.7 (m, C10), 151.7 (s, 4 or 6), 155.5 (s, 4 or 6); $^{31}P\{^1H\}$ NMR (121.5 MHz, CD_2Cl_2): δ 35.9 (d, PhP), 52.3 (br d, *i*Pr$_2$P), $^1J_{PP}$ = 250.3 Hz; ^{31}P NMR (121.5 MHz, CD_2Cl_2): δ 36.0 (m (≈ d), PhP), 52.4 (br m (≈ d), *i*Pr$_2$P), $^1J_{PP}$ = 250.4 Hz; Raman (glass capillary, cm^{-1}): ν 3055 (m), 2940 (m), 2860 (m, νC−H), 2021 (m), 1914 (s, νC−O), 1827 (s, νC−O), 422 (s), 394 (vs), 338 (s); IR (KBr disc, cm^{-1}): ν 3051 (m), 2984 (m), 2935 (m), 2857 (m, νC−H), 2019 (vs), 1912 (vs, br), 1833 (vs, br, νC−O); mp 186−190 °C.

Chlorophosphine Platinum(II) Dichloride 3. **1** (0.20 g, 0.484 mmol) in CH_2Cl_2 (5 mL) was added to $PtCl_2$(cod) (0.18 g, 0.4280.482 mmol) in CH_2Cl_2 (1 mL) at room temperature, and the mixture was stirred for 5 h to give a pale yellow solution. Volatiles were removed in vacuo to give **3** as a pale yellow solid in quantitative yield (0.329 g). Recrystallization from CH_2Cl_2/diethyl ether at 5 °C gave analytically pure material as well as colorless oblong-shaped crystals suitable for X-ray crystallography. EA (%) calcd for $C_{24}H_{27}Cl_3P_2Pt$: C, 42.46; H, 4.01. Found: C, 42.51; H, 4.12. ^1H NMR (300.1 MHz, $CDCl_3$): δ 1.08−1.44 (m, 12H, 4 × *i*Pr CH_3), 3.35−3.63 (m, 6H, 2 × CH_2 and 2 × *i*Pr CH), 7.36−7.46 (m, 4H, *m*-Ph, *p*-Ph and H3), 7.60 (d, 1H, $^3J_{HH}$ = 7.3 Hz, H7), 7.66−7.76 (m, 2H, 2 × *o*-Ph), 7.85 (dd, 1H, $^3J_{HP}$ = 15.0 Hz, $^3J_{HH}$ = 7.5 Hz, H2), 8.07−8.16 (m, 1H, H8); $^{13}C\{^1H\}$ NMR (75.5 MHz, $CDCl_3$): δ 18.7 (d with ^{195}Pt satellites, $^2J_{CP}$ = 2.7 Hz, $^3J_{CPt}$ = 10.3 Hz, *i*Pr CH_3), 19.3 (s with ^{195}Pt satellites, $^3J_{CPt}$ = 11.2 Hz, *i*Pr CH_3), 19.7 (d, $^2J_{CP}$ = 3.0 Hz, 2 × *i*Pr CH_3), 29.0 (d, $^1J_{CP}$ = 35.6 Hz, *i*Pr CH), 30.0 (d, $^1J_{CP}$ = 36.2 Hz, *i*Pr CH), 30.6 (s, CH_2), 30.8 (s, CH_2), 109.5−110.5 (m, C1), 115.8−116.9 (m, C9), 120.1 (d, $^3J_{HH}$ = 9.0 Hz, H7), 120.8 (d, $^3J_{HH}$ = 11.0 Hz, H3), 128.5 (d, $^2J_{CP}$ = 13.6 Hz, *o*-Ph), 131.7 (s, *m*-Ph), 131.9 (s, *p*-Ph), 133.6 (s, C5 or C10), 134.5 (s, C5 or C10), 135.6 (d with ^{195}Pt satellites, $^2J_{CP}$ = 3.3 Hz, $^3J_{CPt}$

dx.doi.org/10.1021/ic501142v | Inorg. Chem. 2014, 53, 8538−8547

Table 4. Crystallographic Data for 2·THF, 3, 4·2CH_2Cl_2, 5·2CH_2Cl_2, and 6·MeCN

	2·THF	3	4·2CH_2Cl_2	5·2CH_2Cl_2	6·MeCN
chemical formula	$C_{32}H_{35}ClMoO_5P_2$	$C_{24}H_{27}Cl_3P_2Pt$	$C_{52}H_{58}Cl_8F_6O_6P_4Pt_2S_2$	$C_{50}H_{58}Cl_6P_4Pd_2$	$C_{26}H_{37}B_2NP_2$
formula weight	692.97	678.87	1754.84	1208.42	447.15
crystal dimensions (mm)	0.02 × 0.02 × 0.02	0.10 × 0.10 × 0.10	0.12 × 0.06 × 0.02	0.10 × 0.03 × 0.03	0.15 × 0.15 × 0.15
crystal system	monoclinic	monoclinic	triclinic	triclinic	triclinic
space group	$P12_1/n1$	$P2_1/c$	$P-1$	$P-1$	$P-1$
a (Å)	14.366(5)	9.551(2)	8.540(1)	8.6966(7)	9.655(1)
b (Å)	15.080(4)	15.931(4)	12.702(2)	12.2811(11)	10.985(2)
c (Å)	15.778(5)	16.866(5)	15.366(2)	12.9710(11)	13.165(2)
α (deg)	90.0000		102.196(8)	90.806(7)	91.411(6)
β (deg)	114.186(8)	100.242(7)	101.379(7)	103.380(8)	99.081(7)
γ (deg)	90.0000		106.672(8)	109.196(8)	110.846(8)
V (Å^3)	3118.2(16)	2525.5(11)	1500.3(4)	1266.7(2)	1283.6(3)
Z	4	4	1	1	2
D_{calc} (g cm^{-3})	1.476	1.785	1.942	1.584	1.157
μ (cm^{-1})	6.470	59.876	52.373	11.87	1.830
no. rflns measured (unique)	19 691 (5677)	15 162 (4419)	11 290 (5242)	12 817 (4593)	8439 (4566)
R_{int}	0.1210	0.0891	0.0508	0.0562	0.0784
R1[a]	0.0606	0.0577	0.0530	0.0529	0.0706
wR2[b]	0.1389	0.2741	0.1431	0.1555	0.1979

[a] $I > 2\sigma(I)$, $R1 = \sum||F_o| - |F_c||/\sum|F_o|$. [b] $wR2 = \{\sum[w(F_o^2 - F_c^2)^2]/\sum w(F_o^2)^2\}^{1/2}$, $w = 1/[\sigma^2(F_o^2) + [(ap)^2 + bp]]$, where $p = [(F_o^2) + 2F_c^2]/3$.

= 22.6 Hz, C8), 139.4 (d, with ^{195}Pt satellites, $^2J_{CP}$ = 7.1 Hz, $^3J_{CPt}$ = 17.5 Hz, C2), 153.4 (s, C4 or C6), 155.5 (s, C4 or C6); $^{31}P\{^1H\}$ NMR (121.5 MHz, $CDCl_3$): δ 12.8 (d with ^{195}Pt satellites, $^1J_{PPt}$ = 3201 Hz, iPr$_2$P), 41.9 (d, $^1J_{PPt}$ = 3836 Hz, PhP(Cl)), $^2J_{PP}$ = 26.4 Hz; ^{31}P NMR (121.5 MHz, $CDCl_3$): δ 12.8 (br s with ^{195}Pt satellites, $^1J_{PPt}$ = 3201 Hz, iPr$_2$P), 41.9 (m, $^1J_{PPt}$ = 3836 Hz, PhP(Cl)); $^{195}Pt\{^1H\}$ NMR (58.1 MHz, $CDCl_3$): δ −4326 (dd, $^1J_{PtP}$ = 3835 Hz, $^1J_{PtP}$ = 3200 Hz); Raman (glass capillary, cm^{-1}): ν 3062 (m), 2931 (m, υC−H); IR (KBr disc, cm^{-1}): ν 2961 (m), 2923 (m, υC−H), 1600 (s); MS (ES+): m/z 696.72 (M − Cl + MeO + Na), 638.76 (M − 2Cl + MeO), 558.83, 516.80, 408.96, 338.99; mp 151−154 °C.

Platinum(II) Dimer ***4***. Me_3SiOTf (0.10 mL, 0.553 mmol) was added to **1** (0.20 g, 0.484 mmol) in CH_2Cl_2 (5 mL) at −78 °C, and the resulting solution was allowed to warm to room temperature and stirred for 2 h. Volatiles were removed in vacuo, and the resulting colorless oil was dried in vacuo for another 1 h to remove the residual Me_3SiCl. A $^{31}P\{^1H\}$ spectrum was collected (in CD_3CN) at this stage, which showed that only the anion was displaced (for OTf^-) because the spectrum was identical to that of the chloride salt **1**.

The oil was dissolved in CH_2Cl_2 (5 mL) and added dropwise to $PtCl_2$(cod) (0.16 g, 0.428 mmol) in CH_2Cl_2 (1 mL) at room temperature, and the pale yellow solution was stirred for 16 h. The solution was layered with hexane (7 mL), which precipitated **4** as a microcrystalline solid (0.363 g, 94.8% yield) and also gave some colorless oblong-shaped crystals suitable for X-ray crystallography. The white solid was isolated by filtration; the material was of analytical purity after washing with CH_2Cl_2 (1 mL) and drying in vacuo. EA (%) calcd for $C_{50}H_{54}Cl_4F_6O_6P_4Pt_2S_2$: C, 37.89; H, 3.43. Found: C, 37.76; H, 3.52; $^{31}P\{^1H\}$ NMR (162.0 MHz, CD_2Cl_2): δ 11.3 (d with ^{195}Pt satellites, $^1J_{PPt}$ = 3409 Hz, iPr$_2$P), 38.5 (d with ^{195}Pt satellites, $^1J_{PPt}$ = 3582 Hz, PhP(Cl)), $^2J_{PP}$ = 28.0 Hz; IR (KBr disc, cm^{-1}): ν 2998(m), 2994 (m, υC−H), 1451 (vs, br), 1033 (s, br), 1099 (vs), 527 (s); MS (ES+): m/z 683.2 (dication + MeCN), 665.2, 642.0 (dication), 624.2, 588.2; HRMS (ES+) calcd for $C_{48}H_{54}Cl_4P_4Pt_2^{2+}$, 642.0613; found, 642.0616; mp 99−103 °C.

Palladium Dimer ***5***. **1** (0.20 g, 0.484 mmol) in CH_2Cl_2 (5 mL) was added to [$Pd_2(dba)_3$] (0.25 g, 0.242 mmol) in CH_2Cl_2 at −78 °C. The resulting suspension was allowed to warm to room temperature and stirred for 16 h to give a dark orange/brown solution. Half of the solvent was removed in vacuo, and a bright yellow solid precipitated after cooling the resulting solution to 2 °C. The yellow powder **5** was collected by filtration and was dried in vacuo (47 mg, 19%). Crystals suitable for X-ray crystallography were obtained from CH_2Cl_2/diethyl ether. EA (%) calcd for $C_{48}H_{54}Cl_2P_4Pd_2$: C, 55.51; H, 5.24. Found: C, 55.48; H, 5.28; ^{1}H NMR (300.1 MHz, $CDCl_3$): δ 0.49−0.70 (m, 12H, 4 × iPr CH$_3$), 0.80−0.90 (m, 6H, 2 × iPr CH$_3$), 1.43−1.53 (m, 6H, 2 × iPr CH$_3$), 2.44−2.61 (br m, 2H, 2 × iPr CH), 3.06−3.18 (m, 2H, 2 × iPr CH), 3.49−3.54 (br m, 8H, 4 × CH$_2$), 6.95−7.01 (m, 6H, Ar CH), 7.20−7.26 (m, 3H, 3 × Ar CH), 7.38 (d, 3H, J = 7.5 Hz, 3 × Ar CH), 7.60−7.69 (m, 12H, 4 × Ar CH + 8 × dba CH), 9.61 (dd, 2H, $^3J_{HP}$ = 8.4 Hz, $^3J_{HH}$ = 7.3 Hz, 2 × o-Ph CH); $^{13}C\{^1H\}$ NMR (67.9 MHz, $CDCl_3$): δ 15.4−16.1 (m, 3 × iPr CH$_3$), 19.6−20.3 (m, 5 × iPr CH$_3$), 30.2−31.0 (m, 3 × CH$_2$), 31.3 (s, CH$_2$), 119.4 (s, C2 or C8), 120.3 (s, C2 or C8), 127.5−128.4 (m, 10 × Ph CH), 132.9 (s, C3 or C7), 133.8 (s, C3 or C7), 138.7 (s, q-C), 151.2 (s, 4 or 6), 156.9 (s, 4 or 6); $^{31}P\{^1H\}$ NMR (121.5 MHz, $CDCl_3$): AA′XX′ spin system (A/A′ = PiPr$_2$, X/X′ = PPh) δ 14.7 (m, A/A′), −176.6 (m, X/X′, *trans*-$^2J_{AX}$ = 322.0 Hz, *cis*-$^2J_{AX}$ = 140.0 Hz, $^2J_{XX'}$ = 4.6 Hz, $^4J_{AA'}$ = 2.2 Hz); MS (ES+): m/z 1018.91 (M − Cl + OH$_2$), 789.06, 659.25, 489.29, 334.16 (ligand − iPr), 318.14; mp 225−229 °C.

Bis(borane) Adduct ***6***. $BH_3{\cdot}SMe_2$ (0.2 mL, 94%, 1.98 mmol) was added to **1** (0.2 g, 0.484 mmol) in THF (5 mL) at −78 °C. The resulting solution was allowed to warm to room temperature and stirred for 2 h. Volatiles were removed in vacuo (without external heating to prevent thermolysis) to give **6** as a yellow oil in quantitative yield (0.196 g). Yellow cube-shaped crystals suitable for X-ray crystallography were grown from MeCN at −5 °C. ^{1}H NMR (400.1 MHz, $CDCl_3$): δ 0.94 (dd, 3H, $^3J_{HP}$ = 16.0 Hz, $^3J_{HH}$ = 6.9 Hz, iPr CH$_3$), 1.10 (dd, 3H, $^3J_{HP}$ = 16.0 Hz, $^3J_{HH}$ = 7.2 Hz, iPr CH$_3$), 1.33−1.43 (m, 6H, 2 × iPr CH$_3$), 2.80−3.05 (m, 2H, 2 × iPr CH), 3.44 (br s, 4H, 2 × CH$_2$), 7.47 (broadened d of m, 1H, $^1J_{HP}$ = 376 Hz, P−H), 7.31−7.48 (m, 7H, H3 + H7 + 5× Ph CH), 7.99 (dd, 1H, $^3J_{HP}$ = 16.0 Hz, $^3J_{HH}$ = 7.5 Hz, H2), 8.28 (dd, 1H, $^3J_{HP}$ = 16.0 Hz, $^3J_{HH}$ = 7.4 Hz, H8); $^{13}C\{^1H\}$ NMR (75.5 MHz, $CDCl_3$): δ 17.8 (s, iPr CH$_3$), 18.4 (s, iPr CH$_3$), 18.6 (s, iPr CH$_3$), 19.5 (s, iPr CH$_3$), 24.4 (d, $^1J_{CP}$ = 30.1 Hz, iPr CH), 25.5 (d, $^1J_{CP}$ = 29.3 Hz, iPr CH), 30.2 (s, CH$_2$), 30.5 (s, CH$_2$), 120.2 (d, $^3J_{CP}$ = 11.6 Hz, C3 or C7), 120.7 (d, $^3J_{CP}$ = 14.3 Hz, C3 or C7), 129.3 (d, $^3J_{CP}$ = 10.2 Hz, m-Ph), 131.7 (d, $^4J_{CP}$ = 2.2 Hz, p-Ph), 133.2 (d, $^2J_{CP}$ = 9.1 Hz, o-Ph), 139.2 (d, $^2J_{CP}$ = 16.6 Hz, C2), 142.1 (d, $^2J_{CP}$ = 11.3 Hz, C8), 152.9 (C4 or C6), 153.5 (C4 or C6); $^{31}P\{^1H\}$ NMR (162.0 MHz, $CDCl_3$): δ −6.6 (br s, PhP(H)), 39.4 (br s, iPr$_2$P); ^{31}P NMR (162.0 MHz, $CDCl_3$): δ −6.6 (br d, $^1J_{PH}$ = 376 Hz, PhP(H)), 39.5 (br s, iPr$_2$P); ^{11}B NMR (128.4 MHz, $CDCl_3$): δ −39.3 (br s, 2 × BH_3); Raman (glass capillary, cm^{-1}): ν 3063 (m), 2935 (s, υC−H), 2352 (m, υP−H), 1318 (s); IR (KBr disc, cm^{-1}): ν 2968 (m), 2931 (m, υC−H), 2389 (s, υP−H); MS (ES+): 377.14 (M − H −

dx.doi.org/10.1021/ic501142v | Inorg. Chem. 2014, 53, 8538−8547

$2BH_3$), 391.16 (−H − BH_3), 407.15 (M − H − BH_3 + O), 421.16 (M − BH_3 + H^+), 753.15; HRMS calcd for $C_{24}H_{30}BP_2$, 391.1916; found, 391.1907; mp 69−72 °C with decomposition.

X-ray Experimental. Table 4 lists details of data collections and refinements. Data for compounds **2**, **3**, and **6** were collected at −180(1) °C by using a Rigaku MM007 high-brilliance RA generator and Mercury CCD system using ω and φ scans. Data for compounds **4** and **5** were collected at −180(1) °C by using a Rigaku MM007 high-brilliance RA generator with a Saturn 70 CCD area detector using ω scans. All instruments use Mo Kα radiation (λ = 0.71075 Å). Intensities were corrected for Lorentz polarization and for absorption. The structures were solved by direct methods. Refinements were done by full-matrix least-squares based on F^2 using SHELXTL.[34] CCDC 1003431−1003435 contain the supplementary crystallographic data for this article. These data can be obtained free of charge via www.ccdc.cam.ac.uk/data_request/cif, by emailing data_request@ccdc.cam.ac.uk, or by contacting The Cambridge Crystallographic Data Centre, 12 Union Road, Cambridge CB2 1EZ, UK; fax: +44 1223 336033. Ellipsoids in all ORTEPs are drawn with 50% probability.

Computational Details. Geometries were fully optimized at the B3LYP/6-31G+* level[35] of density functional theory (DFT), together with a fine integration grid (75 radial shells with 302 angular points per shell). Where available, solid-state structures were used as starting points for the optimizations. The nature of the minima was verified by computations of the harmonic frequencies at the same level of theory. Atomic charges and Wiberg bond indices (WBIs)[36] were computed in a natural population analysis,[37] followed by evaluation of the localized natural bond orbitals (NBOs). All computations were performed using the Gaussian03 suite of programs.[38]

■ ASSOCIATED CONTENT

Ⓢ Supporting Information

Crystallographic data in CIF format. This material is available free of charge via the Internet at http://pubs.acs.org.

■ AUTHOR INFORMATION

Corresponding Author

*E-mail: pk7@st-andrews.ac.uk. Fax: +44 1334 463384. Phone: +44 1334 7304.

Notes

The authors declare no competing financial interest.

■ ACKNOWLEDGMENTS

We thank C.E.R. Horsburgh at the University of St. Andrews and the National Mass Spectrometry Service Center at the University of Swansea for measurement of mass spectra, and we thank the EPSRC, the COST actions CM1302 SIPs, and CM0802 PhoSciNet for financial support. M.B. thanks the School of Chemistry and EaStCHEM for support and for access to a computing facility maintained by H. Früchtl.

■ REFERENCES

(1) Issleib, K.; Seidel, W. *Chem. Ber.* **1959**, *92*, 2681−3008.

(2) (a) Seidel, W. *Z. Anorg. Allg. Chem.* **1964**, *330*, 141−150. (b) Spangenberg, S. F.; Sisler, H. H. *Inorg. Chem.* **1969**, *8*, 1006−1010. (c) Summers, J. C.; Sisler, H. H. *Inorg. Chem.* **1970**, *9*, 862−869.

(3) Schultz, C. W.; Parry, R. W. *Inorg. Chem.* **1976**, *15*, 3046−3050.

(4) Cowley, A. H.; Lattman, M.; Wilburn, J. C. *Inorg. Chem.* **1981**, *20*, 2916−2919.

(5) Baxter, S. G.; Collins, R. L.; Cowley, A. H.; Sena, F. C. *Inorg. Chem.* **1983**, *22*, 3475−3479.

(6) Abrams, M. B.; Scott, B. L.; Baker, R. T. *Organometallics.* **2000**, *19*, 4944−4956.

(7) For recent reviews, see (a) Dyker, C. A.; Burford, N. *Chem.—Asian J.* **2008**, *3*, 28−36. (b) Burford, N.; Ragogna, P. J. *Dalton Trans.* **2002**, 4307−4315. (c) Ellis, B. D.; Macdonald, C. L. B. *Coord. Chem. Rev.* **2007**, *251*, 936−973. Also, see (d) Chitnis, S. S.; MacDonald, E.; Burford, N.; Werner-Zwanziger, U.; McDonald, R. *Chem. Commun.* **2012**, *48*, 7359−7361.

(8) (a) Dyker, C. A.; Burford, N.; Lumsden, M. D.; Decken, A. *J. Am. Chem. Soc.* **2006**, *128*, 9632−9633. (b) Carpenter, Y.; Dyker, C. A.; Burford, N.; Lumsden, M. D.; Decken, A. *J. Am. Chem. Soc.* **2008**, *130*, 15732−15741. (c) Burford, N.; Dyker, C. A.; Decken, A. *Angew. Chem., Int. Ed.* **2005**, *44*, 2364−2367.

(9) (a) Dyker, C. A.; Riegel, S. D.; Burford, N.; Lumsden, M. D.; Decken, A. *J. Am. Chem. Soc.* **2007**, *129*, 7464−7474. (b) Riegel, S. D.; Burford, N.; Lumsden, M. D.; Decken, A. *Chem. Commun.* **2007**, 4668−4670. (c) Weigand, J. J.; Burford, N.; Davidson, R. J.; Cameron, T. S.; Seelheim, P. *J. Am. Chem. Soc.* **2009**, *131*, 17943−17953. (d) Weigand, J. J.; Burford, N.; Lumsden, M. D.; Decken, A. *Angew. Chem., Int. Ed.* **2006**, *45*, 6733−6737.

(10) (a) Weigand, J. J.; Riegel, S. D.; Burford, N.; Decken, A. *J. Am. Chem. Soc.* **2007**, *129*, 7969−7976. (b) Somisara, D. M. U. K.; Buehl, M.; Lebl, T.; Richardson, N. V.; Slawin, A. M. Z.; Woollins, J. D.; Kilian, P. *Chem.—Eur. J.* **2011**, *17*, 2666−2677.

(11) (a) Burford, N.; Cameron, T. S.; Ragogna, P. J. *J. Am. Chem. Soc.* **2001**, *123*, 7947−7948. (b) Slattery, J. M.; Fish, C.; Green, M.; Hooper, T. N.; Jeffery, J. C.; Kilby, R. J.; Lynam, J. M.; McGrady, J. E.; Pantazis, D. A.; Russell, C. A.; Willans, C. E. *Chem.—Eur. J.* **2007**, *13*, 6967−6974.

(12) Ernst, L.; Jones, P. G.; Look-Herber, P.; Schmutzler, R. *Chem. Ber.* **1990**, *123*, 35−43.

(13) (a) Ernst, L.; Look-Herber, P.; Schmutzler, R.; Schomburg, D. *Polyhedron* **1989**, *8*, 2485−2494. (b) Look, P.; Schmutzler, R.; Goodfellow, R. J.; Murray, M.; Schomburg, D. *Polyhedron* **1988**, *7*, 505−511.

(14) Day, G. S.; Pan, B.; Kellenberger, D. L.; Foxman, B. M.; Thomas, C. M. *Chem. Commun.* **2011**, 3634−3636.

(15) Pan, B.; Xu, Z.; Bezpalko, M. W.; Foxman, B. M.; Thomas, C. M. *Inorg. Chem.* **2012**, *51*, 4170−4179.

(16) Pan, B.; Evers-McGregor, D. A.; Bezpalko, M. W.; Foxman, B. M.; Thomas, C. M. *Inorg. Chem.* **2013**, *52*, 9583−9589.

(17) Shaughnessy, K. H. *Chem. Rev.* **2009**, 643−710.

(18) Snelders, D. J. M.; van Koten, G.; Klein Gebbink, R. J. M. *Chem.—Eur. J.* **2011**, *17*, 42−57.

(19) Rosenberg, L. *Coord. Chem. Rev.* **2012**, *256*, 606−626.

(20) Kilian, P.; Slawin, A. M. Z.; Woollins, J. D. *Dalton Trans.* **2006**, 2175−2183.

(21) Wawrzyniak, P.; Fuller, A. L.; Slawin, A. M. Z.; Kilian, P. *Inorg. Chem.* **2009**, *48*, 2500−2506.

(22) Ray, M. J.; Slawin, A. M. Z.; Bühl, M.; Kilian, P. *Organometallics* **2013**, *32*, 3481−3492.

(23) The optimized P−P distance, 2.286 Å, is slightly overestimated with respect to that found in the solid, 2.2347(9) Å (see ref 22).

(24) Haaland, A. *Angew. Chem., Int. Ed.* **1989**, *28*, 992−1007.

(25) Pietschnig, R. *J. Organomet. Chem.* **2007**, *692*, 3363−3369.

(26) Cotton, F. A.; Darensbourg, D. J.; Ilsley, W. H. *Inorg. Chem.* **1981**, *20*, 578−583.

(27) Abel, E. W.; Butler, I. S.; Reid, J. G. *J. Chem. Soc.* **1963**, 2068−2070.

(28) Schenk, W. A. *J. Organomet. Chem.* **1976**, *117*, C97−C100.

(29) Chahen, L.; Therrien, B.; Suess-Fink, G. *Acta Crystallogr.* **2007**, *E63*, m1989.

(30) MacInnis, M. C.; McDonald, R.; Turculet, L. *Organometallics* **2011**, 6408−6415.

(31) Rajendran, K. V.; Gilheany, D. G. *Chem. Commun.* **2012**, *48*, 817−819.

(32) (a) Burford, N.; Losier, P.; Sereda, S. V.; Cameron, T. S.; Wu, G. *J. Am. Chem. Soc.* **1994**, *116*, 6474−6475. (b) Burford, N.; Cameron, T. S.; LeBlanc, D. J.; Losier, P.; Sereda, S.; Wu, G. *Organometallics* **1997**, *16*, 4712−4717.

(33) Drew, D.; Doyle, J. R. *Inorg. Synth.* **1972**, *13*, 47−49.

(34) Sheldrick, G. M. *Acta Crystallogr., Sect. A* **2008**, *64*, 112−122.

(35) (a) Becke, A. D. *J. Chem. Phys.* **1993**, *98*, 5648−5642. (b) Lee, C.; Yang, W.; Parr, R. G. *Phys. Rev. B* **1988**, *37*, 785−789.

(36) Wiberg, K. B. *Tetrahedron* **1968**, *24*, 1083−1096.
(37) Reed, A. E.; Curtiss, L. A.; Weinhold, F. *Chem. Rev.* **1988**, *88*, 899−926.
(38) Frisch, M. J.; Trucks, G. W.; Schlegel, H. B.; Scuseria, G. E.; Robb, M. A.; Cheeseman, J. R.; Montgomery, J. A., Jr.; Vreven, T.; Kudin, K. N.; Burant, J. C.; Millam, J. M.; Iyengar, S. S.; Tomasi, J.; Barone, V.; Mennucci, B.; Cossi, M.; Scalmani, G.; Rega, N.; Petersson, G. A.; Nakatsuji, H.; Hada, M.; Ehara, M.; Toyota, K.; Fukuda, R.; Hasegawa, J.; Ishida, M.; Nakajima, T.; Honda, Y.; Kitao, O.; Nakai, H.; Klene, M.; Li, X.; Knox, J. E.; Hratchian, H. P.; Cross, J. B.; Adamo, C.; Jaramillo, J.; Gomperts, R.; Stratmann, R. E.; Yazyev, O.; Austin, A. J.; Cammi, R.; Pomelli, C.; Ochterski, J. W.; Ayala, P. Y.; Morokuma, K.; Voth, G. A.; Salvador, P.; Dannenberg, J. J.; Zakrzewski, V. G.; Dapprich, S.; Daniels, A. D.; Strain, M. C.; Farkas, O.; Malick, D. K.; Rabuck, A. D.; Raghavachari, K.; Foresman, J. B.; Ortiz, J. V.; Cui, Q.; Baboul, A. G.; Clifford, S.; Cioslowski, J.; Stefanov, B. B.; Liu, G.; Liashenko, A.; Piskorz, P.; Komaromi, I.; Martin, R. L.; Fox, D. J.; Keith, T.; M. A. Al-Laham, Peng, C. Y.; Nanayakkara, A.; Challacombe, M.; Gill, P. M. W.; Johnson, B.; Chen, W.; Wong, M. W.; Gonzalez, C.; Pople, J. A. *Gaussian 03*; Gaussian, Inc.: Wallingford, CT, 2003.